Research Square

Preprints are preliminary reports that have not undergone peer review.
They should not be considered conclusive, used to inform clinical practice,
or referenced by the media as validated information.

Nutrient Regime Restructures Root Fungal Communities in Hydroponic and Aquaponic Systems

Victor Lobanov

victor.lobanov@gu.se

University of Gothenburg

Aline Brossin

INRAe-PEIMA, UE0937, Fish Farming Systems Experimental Facility

Oliver Körner

Leibniz Institute of Horticultural Sciences

Sylvain Yvorel

INRAe-PEIMA, UE0937, Fish Farming Systems Experimental Facility

Nicolas Larrañaga

INRAe-PEIMA, UE0937, Fish Farming Systems Experimental Facility

Alyssa Joyce

University of Gothenburg

Research Article

Keywords: Aquaponics, Hydroponics, Fungal diversity, ITS metabarcoding, Plant sap analysis, Nutrient film technique, Root microbiome, Soilless cultivation

Posted Date: August 19th, 2026

DOI: https://doi.org/10.21203/rs.3.rs-10501616/v1

License: This work is licensed under a Creative Commons Attribution 4.0 International License.
Read Full License

Additional Declarations: No competing interests reported.

Nutrient Regime Restructures Root Fungal Communities in Hydroponic and Aquaponic Systems

Victor Lobanov[1,*], Aline Brossin[2], Oliver Körner[3], Sylvain Yvorel[2], Nicolas Larrañaga[2], Alyssa Joyce[1]

[1] Department of Conservation, University of Gothenburg, Gothenburg, 40530, Sweden
[2] INRAe-PEIMA, UE0937, Fish Farming Systems Experimental Facility, Sizun, France
[3] Leibniz Institute of Horticultural Sciences, Grossbeeren, Germany
[*] Corresponding author: Victor Lobanov; Email: victor.lobanov@gu.se

Abstract

Background: Aquaponics recirculates aquaculture effluent through plant production systems and is widely assumed to provide a more microbially active nutrient environment than conventional hydroponics. Whether this enrichment extends to root-associated fungal communities, or translates into measurable benefits for plant nutrition and yield, has not been established. We tested the hypothesis that aquaculture-derived water enriches root fungal communities independently of nutrient load, and that any such enrichment shapes plant performance. A factorial greenhouse trial compared four contrasting nutrient regimes: source water (negative control), standard coupled-aquaponics, phosphorus- and potassium-supplemented aquaponics, and mineral hydroponics (positive control). These were applied to three tomato cultivars in nutrient film technique gutters supported by coconut coir growbags. Root-associated bacterial (16S rRNA gene) and fungal (ITS) communities were characterized by amplicon sequencing; amplicon-based community inferences were independently verified by ion-chromatography measurement of plant sap nutrients across three canopy levels and four dates, and by per-plant weekly cumulative fruit yields tracked across the full harvest period.

Results: Hydroponic plants produced the highest cumulative yields and operated at an electrical conductivity approximately four to five times higher than aquaponic treatments (1.78 ± 0.12 vs. 0.37–0.41 mS cm^{-1}). Plant sap nutrient concentrations overlapped across fertilized

treatments despite the EC differential, yet only fertilized systems produced commercially viable yields. Fungal alpha and beta diversity restructured across treatments - supplemented aquaponics yielded the lowest fungal richness while standard aquaponics retained the highest. Aquaponic water alone did not generate greater fungal diversity than hydroponics at equivalent nutrient load. Bacterial communities differentiated less among fertilized systems than fungal communities.

Conclusions: Root-associated fungal assemblages responded more strongly to nutrient origin and supplementation than bacterial communities, but this restructuring did not compensate for yield constraints under low-intensity aquaponic nutrient delivery. Nutrient delivery strategy, rather than biological origin of the water alone, is the primary driver of root microbiome structure in soilless cultivation, with direct implications for nutrient management in aquaponic and hydroponic systems.

Keywords: Aquaponics, Hydroponics, Fungal diversity, ITS metabarcoding, Plant sap analysis, Nutrient film technique, Root microbiome, Soilless cultivation

1. Background

Land suitable for agriculture is finite, and further expansion of cropland and associated infrastructure increasingly competes with urbanization and conservation priorities. Agriculture is already the dominant driver of global land-use change, occupying approximately 37-38% of the Earth's ice-free land surface, while an estimated 75% of terrestrial ecosystems have been significantly altered by human activities (1–3). At the same time, climate change is intensifying heat stress, drought risk, and extreme-weather disruptions that compromise yield stability and product quality in open-field systems, especially for fresh-market crops (4,5). Anthropogenic climate change has already resulted in a ~21% decline in agricultural productivity since 1961

(6). These conditions have created strong incentives to shift a larger share of high-value horticultural output into controlled-environment agriculture (CEA).

The past 40 years have seen widespread improvements to yield, quality, and resource-use efficiency for modern CEA systems (7), most of which are entirely soilless (hydroponics) (8). Enclosing plants in controlled environments expands the growing season as well as reduces harvest variability caused by biotic and abiotic stresses (9,10). Closed-loop water and nutrient management lowers overall environmental losses relative to open-field cultivation (8). However, the highly managed and often mineral-based nature of conventional CEA systems is frequently associated with simplified root-zone microbial communities and reduced biological diversity (11–13), which may limit nutrient transformation processes, plant-microbe interactions, and the expression of secondary metabolites in crops.

In this context, aquaponics represents a biologically enriched variant of hydroponics that partially addresses these limitations. Although aquaponic systems exhibit substantial diversity in design and operation, they uniformly promote microbial communities that play a crucial role in the local carbon and nitrogen cycles and the solubilization of mineral nutrients (14–17). Taxonomic studies have revealed that aquaponic systems host diverse bacterial assemblages shaped by system design, fish stocking density, and nutrient management strategy (18–24). The result is a nutrient environment that is chemically more heterogeneous and biologically more complex than conventional mineral-based hydroponic solutions, while retaining the spatial efficiency and environmental control characteristic of CEA systems.

However, optimal nutrient management in aquaponics remains disputed, particularly whether greater microbial diversity can improve plant nutrient acquisition enough to compensate for the lower dissolved nutrient concentrations typically found in aquaponic systems compared with hydroponics (25–34). Comparatively little attention has been paid to fungal communities within aquaponic systems, despite their established roles in organic matter decomposition,

nutrient mobilization, and plant-microbe interactions in soil and soilless environments (35–40). Because nutrient recommendations for soilless cultivation are largely derived from mineral hydroponic benchmarks (41), supplementation strategies in aquaponics are often implemented empirically, without explicit consideration of microbially mediated nutrient transformations. Across the existing literature, there is still no clear consensus on whether microbially enriched aquaponic nutrient regimes can consistently match hydroponic productivity under comparable management intensity.

Consequently, root-associated fungal diversity in aquaponic systems remains poorly characterized, and no integrated framework currently links fungal community composition with nutrient delivery regime, plant nutritional status, and yield performance. No study has yet combined measurements of aqueous nutrient availability, nutrient uptake within plant tissues, harvest outcomes, and root-associated microbial - particularly fungal - diversity across contrasting soilless nutrient regimes. This gap limits the ability to assess whether biological complexity can meaningfully offset lower dissolved nutrient concentrations without compromising yield or system control.

The present study investigated the relationships between nutrient delivery strategy, plant nutritional status, yield performance, and microbial community structure in both hydroponic and aquaponic systems. Specifically, this work aimed (i) to quantify nutrient uptake dynamics of tomato plants under contrasting nutrient densities and origins, and (ii) to produce the first detailed map of fungal diversity in hydroponic and aquaponic rooting environments. By explicitly linking nutrient availability, internal plant nutrient storage, yield outcomes, and fungal community composition, this study provides a systems-level framework for re-evaluating nutrient management strategies in biologically active soilless cultivation.

2. Methods

2.1. Experimental design and treatments

The greenhouse trial was conducted at the INRAe-PEIMA Fish Farming Systems Experimental Facility (UE0937, Sizun, France). To evaluate the effects of contrasting nutrient regimes, four treatments were established: (i) source water with no nutrient addition (negative control); (ii) a hydroponic nutrient solution (positive control) prepared using the Flora Series (Flora Micro, Flora Grow, and Flora Bloom; General Hydroponics, Sebastopol, USA) dosed according to the manufacturer's specifications; (iii) aquaponic water consisting solely of aquaculture effluent; and (iv) supplemented aquaponic water, in which phosphorus and potassium were added to aquaculture effluent using commercial supplements (Canna-P (17% P_2O_5) and Canna-K (16% K_2O); CANNA International B.V., Naaldwijk, Netherlands) to complement nutrient concentrations typically limiting in aquaponic systems. No pH correction was applied to any treatment. Nutrient concentrations varied over the cultivation period and differed among treatments; influent and effluent concentrations are summarized in Figure 1.

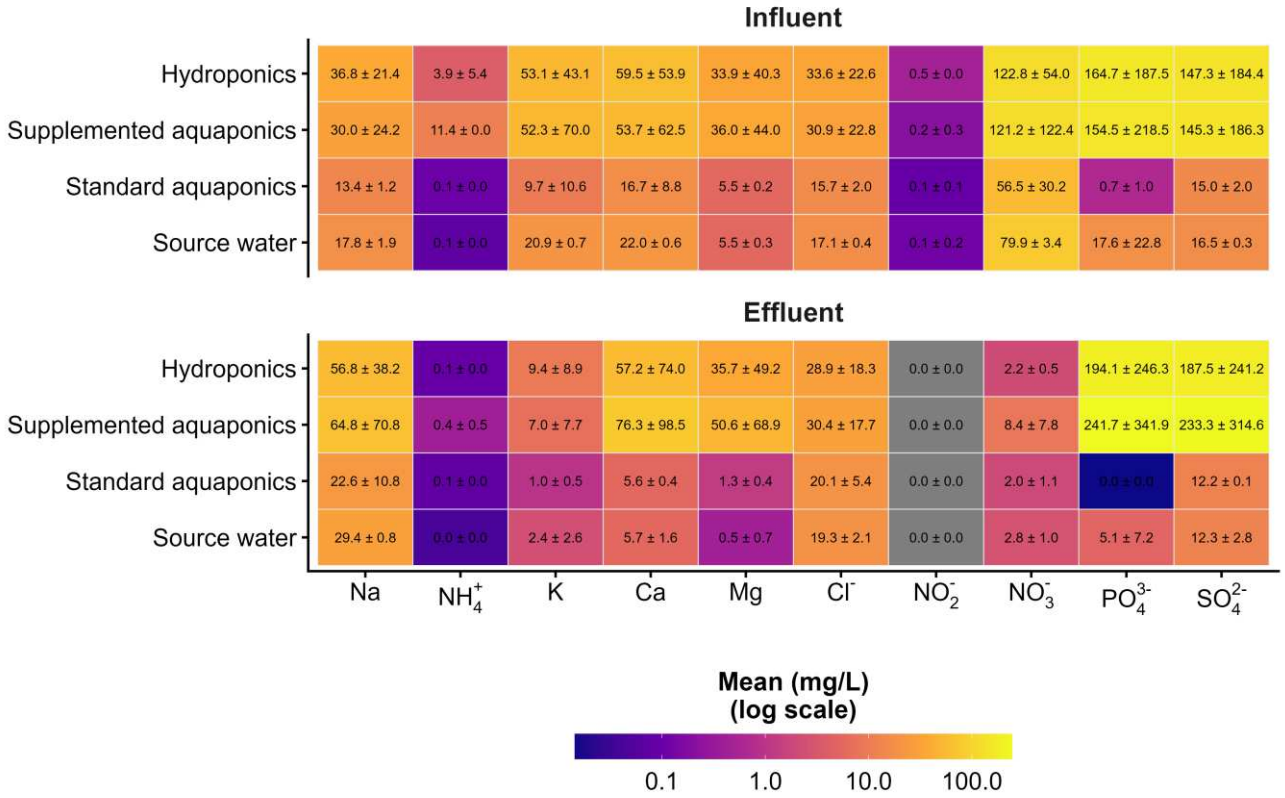


Figure 1. Dissolved inorganic nutrient concentrations across treatments. Values are means (± SD) for influent and effluent waters. Color indicates mean concentration on a $\log_{10}$ scale (mg L^{-1}), and numerical labels show mean ± SD in absolute units.

Each plant was assigned a P-G-N code corresponding to the parcel, gutter, and individual plant (Figure 2). Tomato plants were harvested weekly and provided the plant material used for downstream sap and microbial sequencing analyses. Three tomato cultivars were grown: 'Star Gold', 'Black Cherry', and 'Apéro'.

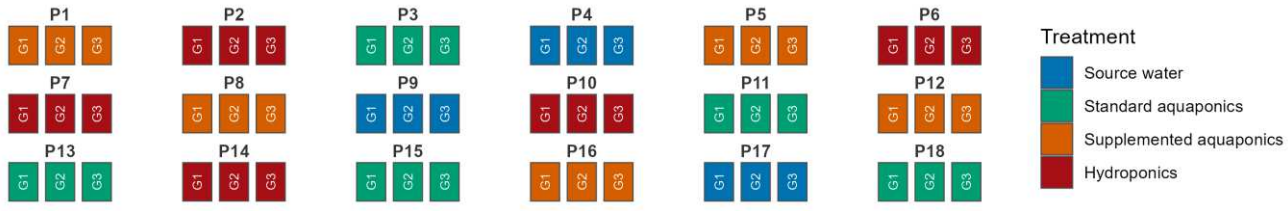


Figure 2. Distribution of treatments within the experimental design.

2.2. Infrastructure and growing conditions

The growing period extended from 2 June to 20 November 2025. Photoperiod ranged from approximately 11 to 16 h during the spring/summer period and declined to approximately 8.5 h by the end of the harvest season. Direct sunlight averaged approximately 5 h day-1 in spring (March-May), 6 h day-1 in summer (June-August), and 4 h day-1 in autumn (September-November); these values represent climatological averages for the site and were not measured *in situ* at the canopy.

Plants were grown in NFT gutters (Goponic, France) used in combination with coconut coir growbags to support root establishment; NFT here describes the recirculating thin-film delivery of nutrient solution along the gutter base rather than a strictly substrate-free configuration. Each gutter measured 4 m in length with a slope of approximately 2.5%. Each gutter held nine plants, and each parcel (approximately 4 m x 85 cm) comprised three gutters (27 plants per parcel). Plants were established in coconut coir growbags (JIFFY 5050, 120 x 15 x 8 cm; a 50/50 mix of coconut pith and husk chips; Jiffy Group, Norway). The substrate had a pH of 5.5-6.5, electrical conductivity of 300 ± 200 μS cm^{-1}, total porosity of 95%, air-filled porosity of 25%, water-holding capacity of 70% (by volume, after drainage), dry bulk density of 68-78 kg m^{-3}, and organic matter content of 96%. Irrigation was delivered via micro-drippers at the base of each plant at a rate of approximately 3 L h^{-1} per plant when activated. Each treatment was supplied from a separate 300-L sump corresponding to each of the four treatments.

Tomato seedlings (non-grafted, grown on rockwool plugs) were obtained from Groupe Thomas Plants (France), grown in the nursery for approximately 28 days, and when the first flower cluster was at the onset of development. Plants were trained to a single stem, with lateral shoots removed at least twice weekly. Pollination was carried out by bumblebees (Biobest, Belgium).

Water quality was monitored weekly for pH and electrical conductivity (EC) using the Hach HQ40d portable multiparameter meter equipped with an IntelliCAL PHC101 pH electrode and

147 an IntelliCAL CDC401 conductivity probe (Hach Lange, USA). The pH was monitored but
148 not chemically adjusted in any treatment; aquaponic and source-water pH was buffered by the
149 recirculating biofilter and source water carbonate chemistry, while drift in the hydroponic
150 treatment reflected uncorrected accumulation typical of recirculating mineral solutions.
151 Temperature and dissolved oxygen were recorded continuously for aquaponic water using an
152 Aqualarm monitoring system (Teraqua). Ammonium (NH_4^+), nitrite (NO_2^-), nitrate (NO_3^-), and
153 orthophosphate (PO_4^{3-}) were measured weekly using Hach Lange photometric test kits (LCK
154 341, LCK 339, LCK 304, and LCK 349, respectively).

155 ***2.2.1. Pest and disease management***

156 An integrated pest management (IPM) program was implemented in collaboration with La
157 Source using Biobest biological control agents. The following measures were deployed two
158 weeks after transplanting: (i) a Delta trap with a *Tuta absoluta* pheromone capsule was
159 positioned at the greenhouse entrance at canopy height and renewed every four weeks; (ii) four
160 yellow sticky traps (Bug-Scan; Biobest) were installed for early detection of whitefly
161 (*Trialeurodes vaporariorum*) and renewed when no longer legible; (iii) six *Macrolophus*
162 *pygmaeus* nursery stations were established on marked tomato plants, with supplemental food
163 applied at canopy height every two weeks; (iv) *Amblyseius cucumeris* sachets (1000 predatory
164 mites each) were deployed for thrips control; and (v) Aphidaxis flasks (a blend of six parasitoid
165 wasp species: *Aphidius colemani*, *A. ervi*, *A. matricariae*, *Aphelinus abdominalis*, *Praon*
166 *volucre*, and *Ephedrus cerasicola*) were released every two weeks for aphid management. A
167 minor whitefly population was detected during the growing season and successfully controlled
168 through additional Bug-Scan traps and the release of *Encarsia formosa*; no crop damage was
169 recorded.

2.3. Plant sap sampling and analysis

Plant sap was analyzed from three canopy levels (low, middle, and high) and from fruit. Leaf positions were indexed from the plant base upward: low = first fully expanded leaf from the bottom, middle = fifth fully expanded leaf, and high = highest fully expanded leaf immediately below the apical meristem. Sampling was carried out over 16 days during the peak of the harvest period (5, 12, 18, and 21 August 2025). All leaf and fruit samples were collected at the same time each morning (ca. 08:00-09:00) and packaged in plastic bags for immediate shipment from the greenhouse site (INRAe-PEIMA, France) to the University of Ghent (Ghent, Belgium). Upon arrival (ca. 24-36 hours later), samples were cleaned by dabbing with paper towels to remove excess moisture or dust. To ensure only sap was collected, leaf laminae were separated from vascular tissue using a scalpel. Samples were then weighed and frozen at -20 C following established protocols (42–45).

A freeze-thaw and centrifugation technique was used for sap extraction. Weighed plant tissue was placed inside a 2 mL Eppendorf tube with 500 µL deionized water, frozen at −20 °C, and thawed 24 hours later to rupture cell walls. Samples were centrifuged at 16,000 ×g for 5 minutes to separate the diluted liquid sap. The supernatant was transferred to a new 2 mL Eppendorf tube and diluted to a final ethanol concentration of 25% to precipitate proteins. After a second centrifugation under identical conditions, the liquid was filtered through a 0.22 µm syringe filter. Samples were capped immediately after filtering and stored at 4 °C prior to analysis.

Water samples were filtered through a 0.22 µm filter and analyzed without additional preparation. In both cases, ions were quantified at the University of Ghent (Ghent, Belgium) by ion exchange chromatography (IC) on a 930 Compact IC Flex system (Metrohm, Switzerland) equipped with a Metrosep A Supp 5 150/4.0 column, a Metrosep A Supp 4/5 Guard column (4.0 mm), and an 850 IC conductivity detector (Metrohm, Switzerland). A 1.7

mM HNO_3 and 1.7 mM 2,6-pyridinedicarboxylic acid solution was used as the mobile phase for cation elution, and a 1.0 mM $NaHCO_3$/3.2 mM Na_2CO_3 solution for anion elution. The following ions were quantified in each sample: Li^+, Na^+, NH_4^+, K^+, Ca^{2+}, Mg^{2+}, Cl^-, NO_2^-, Br^-, NO_3^-, PO_4^{3-}, and SO_4^{2-}.

In addition to IC analysis, pH and electrical conductivity of the water were measured weekly. Nitrate and orthophosphate were measured weekly as part of the standard aquaculture monitoring schedule.

Sap-to-water ratios were calculated per observation and $\log_{10}$-transformed. These ratios were then averaged by treatment, canopy position, nutrient, and sampling date to generate summary matrices for visualization. Heatmaps were used to display mean $\log_{10}$(sap:water) values, faceted by canopy position and treatment.

2.4. Harvest assessment

Harvests were conducted weekly from 18 July 2025 (52 days after transplanting) to 20 November 2025 until fruit production ceased. For each plant and harvest date, the number of fruits and the fresh weight of each individual fruit were recorded. Individual harvest records were aggregated to compute cumulative yield per plant across the entire harvest period. This structure enabled direct comparison of yield performance among nutrient delivery strategies and cultivars. Harvest duration was calculated as days since the first harvest date. For each harvest event, the number of fruits and total fruit mass were computed exclusively from individual fruit weights. Plant-level harvest trajectories were summarized at the gutter level by calculating the mean and standard deviation of cumulative fruit number and mass across plants within each gutter.

For analyses relating plant performance to nutrient status, sap nutrient concentrations were summarized at the plant level as the median across all canopy positions and sampling dates. Water pH and electrical conductivity were matched to sap sampling dates using nearest-date

assignment and summarized per plant as medians across exposure periods. Plants were classified as high-yielding based on a relative yield threshold, defined as ≥90% of the maximum observed yield. For each nutrient and water variable, empirical target ranges were defined as the minimum and maximum predictor values observed among high-yield plants. Outliers in predictor variables were identified within each treatment and predictor using a median absolute deviation (MAD) criterion and excluded only from predictor-yield visualization analyses.

2.5. Sequencing and bioinformatic analysis

At harvest, roots were collected, lightly dried, and stored at −20 °C for later sequencing. Genomic DNA extracts (10 µL per sample) were submitted to LGC Genomics GmbH (Berlin, Germany) for amplicon sequencing. The V3-V4 hypervariable region of the bacterial 16S rRNA gene was amplified using primers 341F (5′-CCTACGGGNGGCWGCAG-3′) and 785Rmod (5′-GACTACHVGGGTATCTAAKCC-3′), following Klindworth et al. (46). For fungal community analysis, the internal transcribed spacer (ITS) region was amplified using primers fITS7 (5′-GARTCATCGAATCTTTG-3′) (47) and ITS4 (5′-TCCTCCGCTTATTGATATGC-3′) (48).

For library preparation, 1 µL of DNA extract was used per PCR reaction. Each 20 µL PCR mixture contained 15 pmol of each primer, MyTaq reaction buffer with 1.5 U MyTaq DNA polymerase (Bioline), and 2 µL BioStabII PCR Enhancer (Sigma). Forward and reverse primers for each sample carried identical, sample-specific 10-nt barcode sequences.

PCR amplification was performed for 30 cycles under the following conditions: initial denaturation at 96 °C for 2 min, followed by cycles of denaturation at 96 °C for 15 s, annealing at 50 °C for 30 s, and extension at 70 °C for 90 s. Amplicon presence and approximate concentration were assessed by agarose gel electrophoresis. Approximately 20 ng of amplicon DNA from each sample were pooled, with up to 48 uniquely barcoded samples per pool.

Amplicon pools were purified using one volume of AMPure XP magnetic beads (Agencourt) to remove primer dimers and short non-specific products, followed by an additional purification step using MinElute columns (Qiagen).

Purified amplicon pools (approximately 100 ng DNA per pool) were used for Illumina library construction via adaptor ligation using the Ovation Rapid DR Multiplex System 1-96 (NuGEN). Libraries were pooled and size-selected by preparative gel electrophoresis prior to sequencing. Paired-end sequencing (2 × 300 bp) was performed on an Illumina NextSeq 2000 platform using a P1 flow cell with XLEAP-SBS chemistry.

Sequence data were processed using the DADA2 pipeline (49), with outputs provided as a processed feature table and associated quality and taxonomic summaries. A phyloseq object was generated to enable downstream statistical and ecological analyses in R (50), and taxonomic composition was visualized using Krona plots (51). Alpha diversity metrics (observed richness, Shannon index, Simpson index) were calculated for each treatment using pooled ASV abundance vectors. These metrics were computed independently for bacterial (16S rRNA gene) communities, the full ITS ASV table (all recovered ITS sequences), and an ITS-derived fungal subset restricted to ASVs assigned to Kingdom Fungi (a taxonomic filter of the ITS data, not a separate amplicon). For beta diversity, bacterial communities and the full ITS and Fungi-only ITS tables were ordinated using Bray–Curtis dissimilarities on relative-abundance-standardized ASV tables followed by principal coordinates analysis (PCoA). Ordination goodness-of-fit was quantified as the Mantel correlation between original Bray–Curtis distances and Euclidean distances in the two-dimensional ordination space. Complementary to the Fungi-only filter, ITS ASVs that lacked a Kingdom assignment (Unassigned) were ordinated separately using Jaccard distances on presence/absence to evaluate whether unclassified sequences also structured by nutrient regime. For interpretation of ITS composition beyond taxonomy, ASVs were assigned to simplified ecological groups at

the class rank by mapping each class to a dominant, well-established ecological strategy reported in the mycological and microbial ecology literature (52). Classes were collapsed to: Chytrids; Fungi (decomposers); Fungi (fast saprotrophs); Fungi (generalists); Fungi (plant-assoc.); Fungi (yeasts); Green algae; Oomycetes; Plant (host); and Other (classes without a single dominant strategy under this scheme). Unclassified or placeholder class labels were retained as Unassigned. This approach assumes that, although ecological roles may vary among species within a class, most classes exhibit a characteristic set of lifestyles sufficiently consistent to support class-level categorical inference; groupings were treated as descriptors of ASV identity rather than as direct functional measurements.

2.6. Correlation and multivariate analyses

Associations between microbial diversity metrics and nutrient variables were evaluated using treatment-level summaries. Sap and water nutrient concentrations were summarized as treatment means, and alpha diversity metrics were correlated with nutrient values using Spearman's rank correlation. For beta diversity, permutational multivariate analysis of variance (PERMANOVA) (53) was conducted on Bray-Curtis distance matrices to test the effects of treatment, sap nutrient variables, and water nutrient variables, individually and in combination. Homogeneity of dispersion was evaluated using betadisper tests. Environmental fitting (envfit) was applied to PCoA ordinations to assess the direction and strength of associations between sap nutrient variables and community composition. All multivariate community analyses were performed using the vegan package (54) in R.

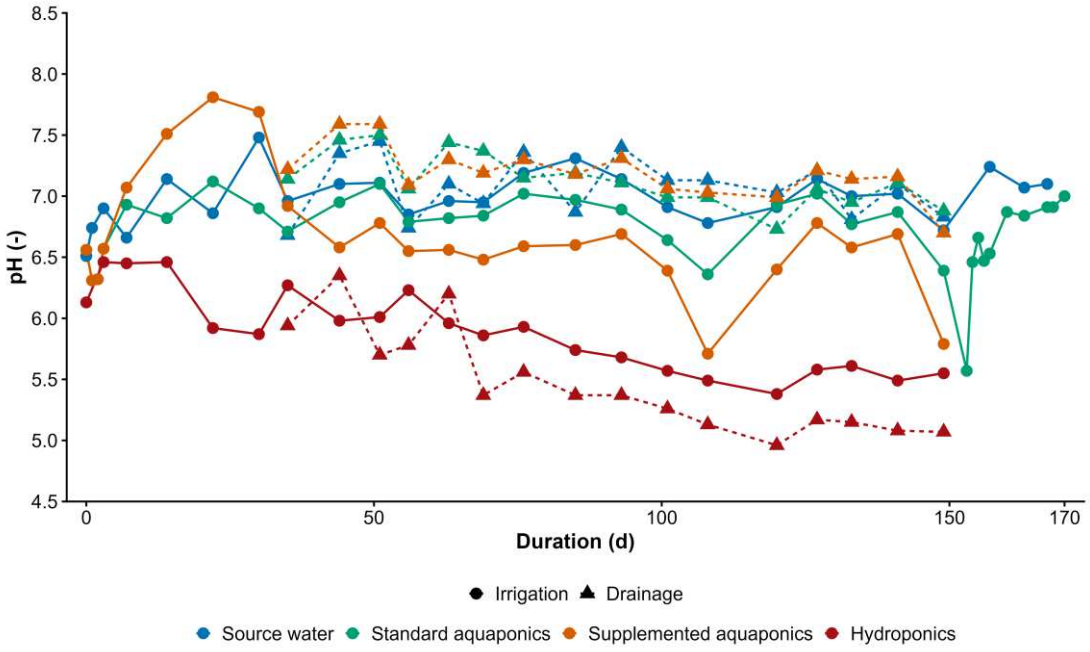
Additional supporting harvest trajectories are provided in Supplementary Figure S2.

3. Results

3.1. Physicochemical parameters

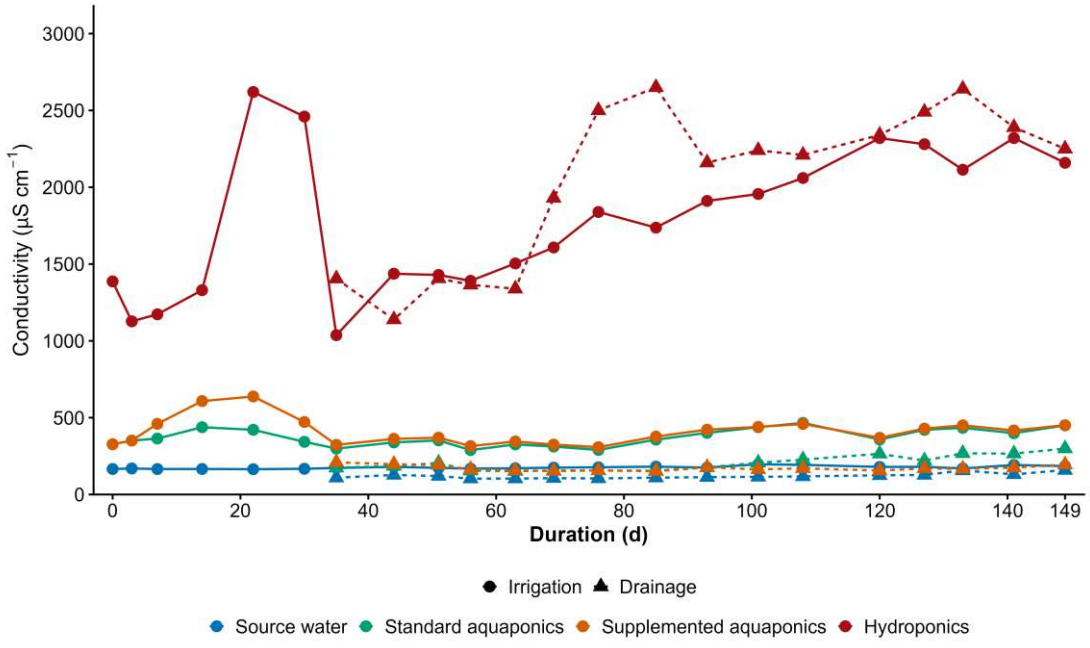
The pH remained comparatively stable in aquaponic and source-water treatments but declined steadily in the hydroponic treatment (Figure 3). Electrical conductivity was also stable within most treatments, although the hydroponic treatment showed greater variance and consistently higher values (Figure 4).

Mean electrical conductivity in the hydroponic treatment (1.78 ± 0.12 mS cm^{-1}) was approximately four to five times higher than in standard aquaponics (0.37 mS cm^{-1}) and supplemented aquaponics (0.41 mS cm^{-1}), while source water maintained the lowest EC values throughout the trial (Figure 4). This separation in ionic strength established the primary nutrient delivery gradient underlying subsequent comparisons of plant performance and microbial community composition. Although the supplemented aquaponic treatment was intended to differ from standard aquaponics only in phosphorus and potassium, weekly fertilizer pulses introduced minor counter-ion shifts (e.g. accompanying SO_4^{2-} and Mg^{2+} from the supplement matrix) and altered the timing of nutrient uptake relative to fish-feed pulses, which together produced small secondary differences in the broader cation/anion profile. The progressive pH decline in the hydroponic treatment is consistent with the acidifying effect of nutrient uptake in mineral solutions, whereas fish-effluent-derived water maintained comparatively stable pH values in aquaponic treatments throughout the cultivation period (Figure 3).



310

311 Figure 3. The pH dynamics in irrigation and drainage water across treatments.



312

313 Figure 4. Electrical conductivity dynamics in irrigation and drainage water across treatments.

3.2. Plant sap analysis

Spatiotemporal patterns of plant sap nutrient composition are expressed relative to water quality across treatments (Figure 5), with plant sap extracted from a representative batch of the tomato cultivars used in the study (Table 1). Table 1 reports the parcel, gutter, and plant-ID coding used for tomato sampling.

Table 1. Summary of plants used for plant sap analysis.

Cultivar	Parcels (P)	Gutters (G)	Plant IDs per gutter (N)
Apéro	2, 9, 13, 16	1, 2	1-4, 6-9
Black Cherry		1, 3	
Star Gold		1, 2, 3	

Four sampling dates were selected during a period when plants were fully mature and actively producing fruit. Nutrient concentrations were measured at multiple canopy positions and normalized by the corresponding treatment-specific mean aqueous nutrient concentration to obtain sap:water (Sap/WQ) ratios. Ratios were $\log_{10}$-transformed, averaged across plants within each canopy level, and displayed as heatmaps by treatment and time point. Colors represent mean $\log_{10}$(Sap/WQ) values, with higher values indicating greater relative enrichment of nutrients in plant sap compared with the surrounding water.

Across treatments and sampling dates, sap:water ratios revealed ion-specific and canopy-dependent enrichment patterns (Figure 5). Calcium was consistently enriched in lower canopy tissues relative to upper canopy levels, while potassium displayed the opposite vertical gradient. These spatial patterns were broadly conserved across treatments, though the magnitude of enrichment differed with nutrient regime. Aquaponic and source water treatments generally exhibited higher sap:water ratios for several ions, reflecting the lower baseline aqueous nutrient concentrations in these treatments rather than higher absolute tissue

accumulation. Temporal variation across the four sampling dates was moderate, indicating that nutrient partitioning patterns remained relatively stable during the peak production period.

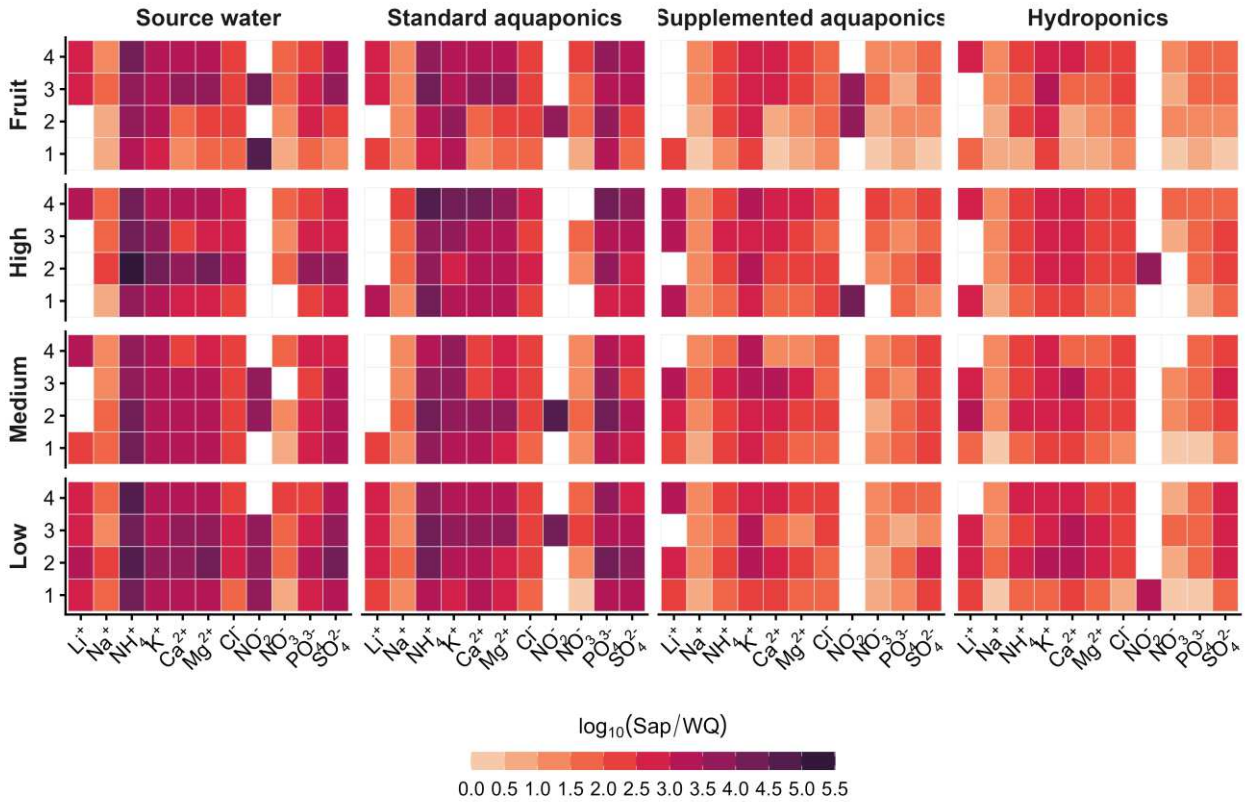


Figure 5. Plant sap:water nutrient ratios across treatments. Heatmaps show $\log_{10}$(sap/water) ion ratios for Li^+, Na^+, NH_4^+, K^+, Ca^{2+}, Mg^{2+}, Cl^-, NO_2^-, NO_3^-, PO_4^{3-}, and SO_4^{2-} at four sampling dates (rows 1–4 within each panel). Row blocks are tissue/canopy positions: Fruit = fruit sap; High = highest fully expanded leaf below the apical meristem; Medium = fifth fully expanded leaf from the base; Low = first fully expanded leaf from the base (Methods). Sap concentrations were normalized to treatment-specific water nutrient concentrations and $\log_{10}$-transformed.

3.3. Harvest outcomes

Harvest performance differed among nutrient regimes (Figure 6). Hydroponic plants produced the greatest number of fruits and the highest total fruit mass, although yields varied substantially among plants. Source-water plants had the lowest fruit number and biomass. Aquaponic treatments produced intermediate yields, with supplemented aquaponics tending toward higher fruit number and biomass than standard aquaponics, although variability remained appreciable.

Within the hydroponic treatment, yield variability among plants was largely attributable to cultivar identity, with distinct cultivar-specific production trajectories evident across the harvest period (Supplementary Figures S1–S2). The two aquaponic treatments exhibited overlapping yield distributions, with supplemented aquaponics showing a trend toward higher cumulative fruit mass that did not consistently exceed standard aquaponics across all cultivars. This pattern suggests that phosphorus and potassium supplementation provided a modest yield benefit under the low-EC conditions characteristic of aquaponic operation, without fully bridging the productivity gap relative to hydroponics. Mean tomato yield in hydroponics was 3,000 ± 890 g per plant.

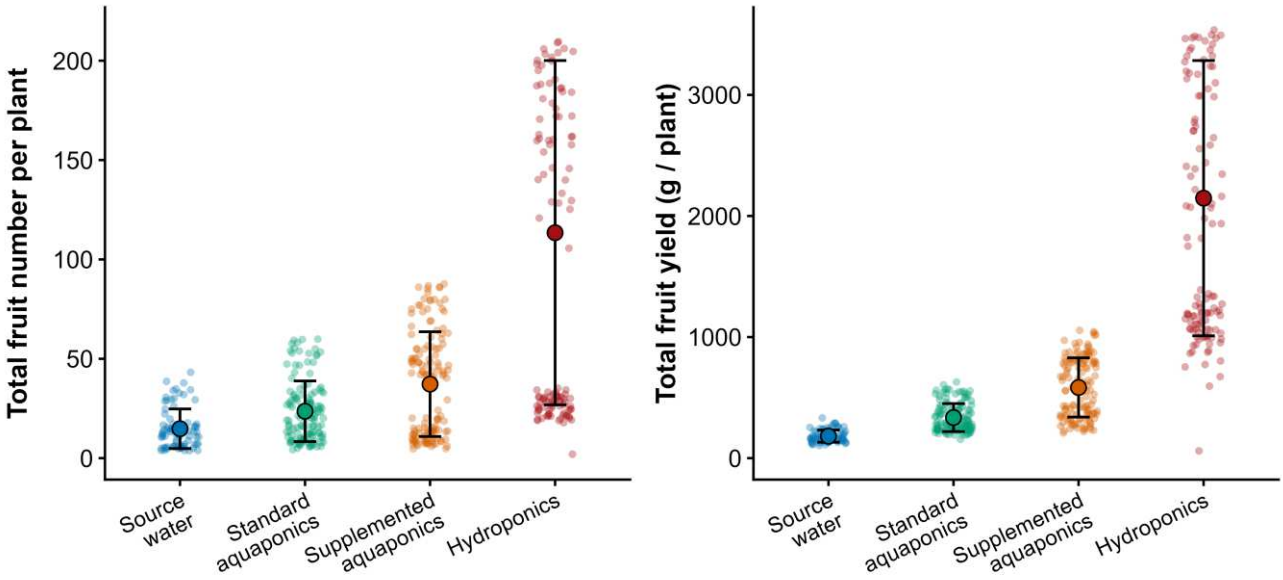


Figure 6. Cumulative fruit number and total fruit yield per plant across nutrient regimes.

Pooled tomato yields across all tomato cultivars for each treatment are reported in Supplementary Figure S1; tomato individual yields (number of fruits and total biomass) are reported in Supplementary Figure S2.

3.4. Rhizobiome diversity metrics

Root microbial communities (the rhizobiome) were analyzed across all treatments. Alpha diversity of bacterial (16S rRNA) and fungal (ITS) communities varied consistently among treatments across all metrics (Figure 7). Supplemented aquaponics exhibited the lowest diversity for both markers, with reduced richness and evenness relative to the other systems. For bacteria, richness was highest in source water and hydroponics, whereas standard aquaponics showed intermediate richness but higher evenness as indicated by Shannon and Simpson indices. Fungal communities displayed a contrasting pattern, with standard aquaponics showing the highest richness and evenness, followed by hydroponics, while source water exhibited comparatively low fungal diversity.

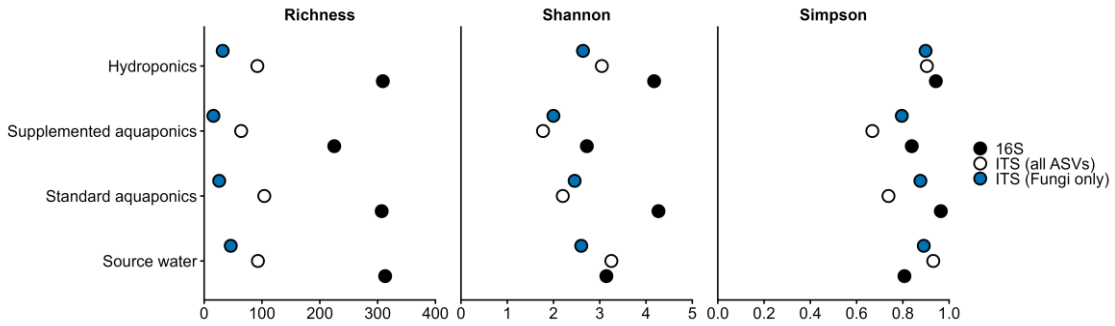


Figure 7. Alpha diversity of bacterial (16S rRNA gene) and ITS communities across treatments. Richness, Shannon, and Simpson diversity are shown for source water, standard aquaponics, supplemented aquaponics, and hydroponics. Within each panel, markers are 16S, the full ITS ASV table (all recovered ITS sequences), and the ITS-derived fungal subset (ASVs assigned to Kingdom Fungi).

Beta diversity ordination revealed clear differences in community composition among nutrient management treatments (Figure 8). Because ITS primers recover a mixed amplicon pool, fungal community structure was examined from the same ITS sequencing run as (i) the full ITS ASV table, (ii) an ITS-derived fungal subset restricted to ASVs assigned to Kingdom Fungi, and (iii) the complementary pool of ITS ASVs that lacked a Kingdom assignment (Unassigned). Bacterial communities were ordinated from the 16S rRNA gene ASV table.

Panels A–C use Bray–Curtis distances on relative abundances; panel D uses Jaccard distances on presence/absence of unassigned ITS ASVs.

Across markers, source water was consistently separated from fertilized systems, indicating that nutrient addition reshaped both bacterial and fungal assemblages relative to the unamended control (Figure 8A–C). Within fertilized systems, bacterial communities (16S) showed comparatively limited differentiation among standard aquaponics, supplemented aquaponics, and hydroponics, whereas fungal communities exhibited stronger treatment separation in both the full ITS table and the Fungi-only subset. Unassigned ITS ASVs likewise structured by treatment (Figure 8D): hydroponics and source water occupied distinct regions of the ordination, while standard and supplemented aquaponics clustered near each other and apart from those two systems. This indicates that system-level differences extended beyond taxa that could be placed in Kingdom Fungi and that the unclassified ITS pool retained treatment-informative composition rather than unstructured noise.

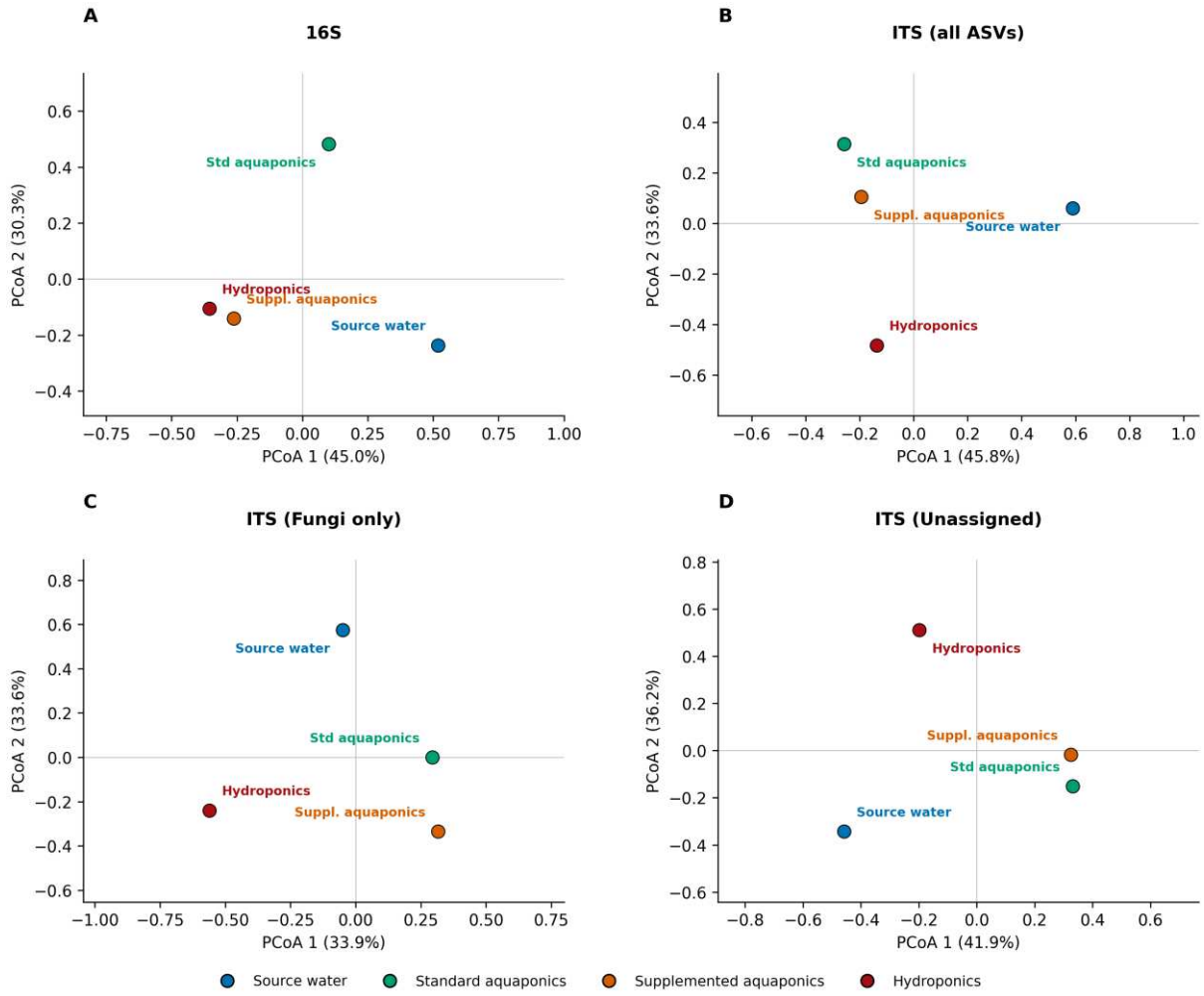


Figure 8. Treatment-level microbial community ordination. (A) 16S rRNA gene ASVs, (B) full ITS ASV table, and (C) ITS-derived fungal subset (Kingdom Fungi) are shown as Bray–Curtis principal coordinates analyses (PCoA). (D) ITS ASVs lacking a Kingdom assignment (Unassigned) are shown as a Jaccard PCoA on presence/absence. Panels B–D use the same ITS amplicon run; C and D are complementary taxonomic filters of that dataset, not independent markers. Each point is the treatment-aggregated community for source water, standard aquaponics, supplemented aquaponics, and hydroponics; axis labels report the percentage of variance explained by each principal coordinate.

ASVs were classified from 16S rRNA gene and ITS metabarcoding datasets (Figures 9 and 10). Each bar represents 100% of the unique ASVs detected within a treatment at the class rank, with colored segments indicating the proportional contribution of individual classes. Numbers in parentheses in the legend denote the total number of unique ASVs assigned to each

class across all treatments combined. ASVs that could not be confidently classified at the class level are grouped as Unassigned.

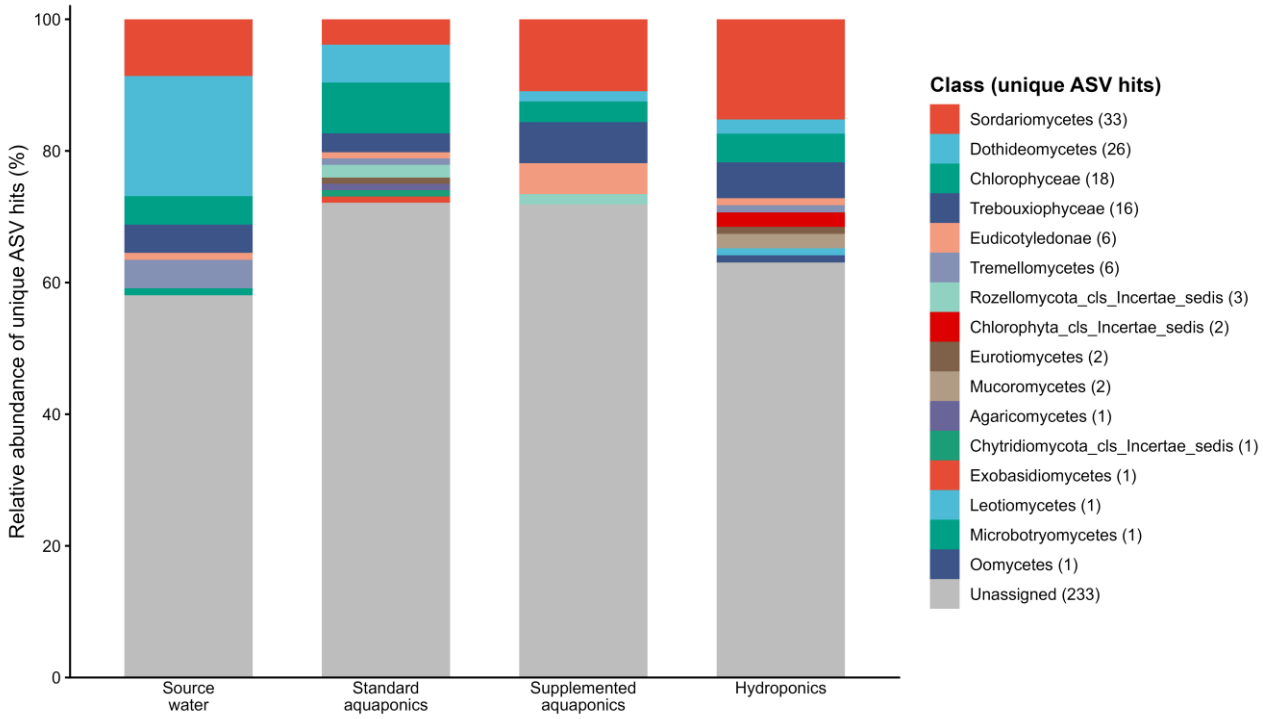


Figure 9. ITS class-level ASV composition by treatment. Stacked bar charts show the relative abundance of unique ASV hits (%) assigned to ITS class for each treatment.

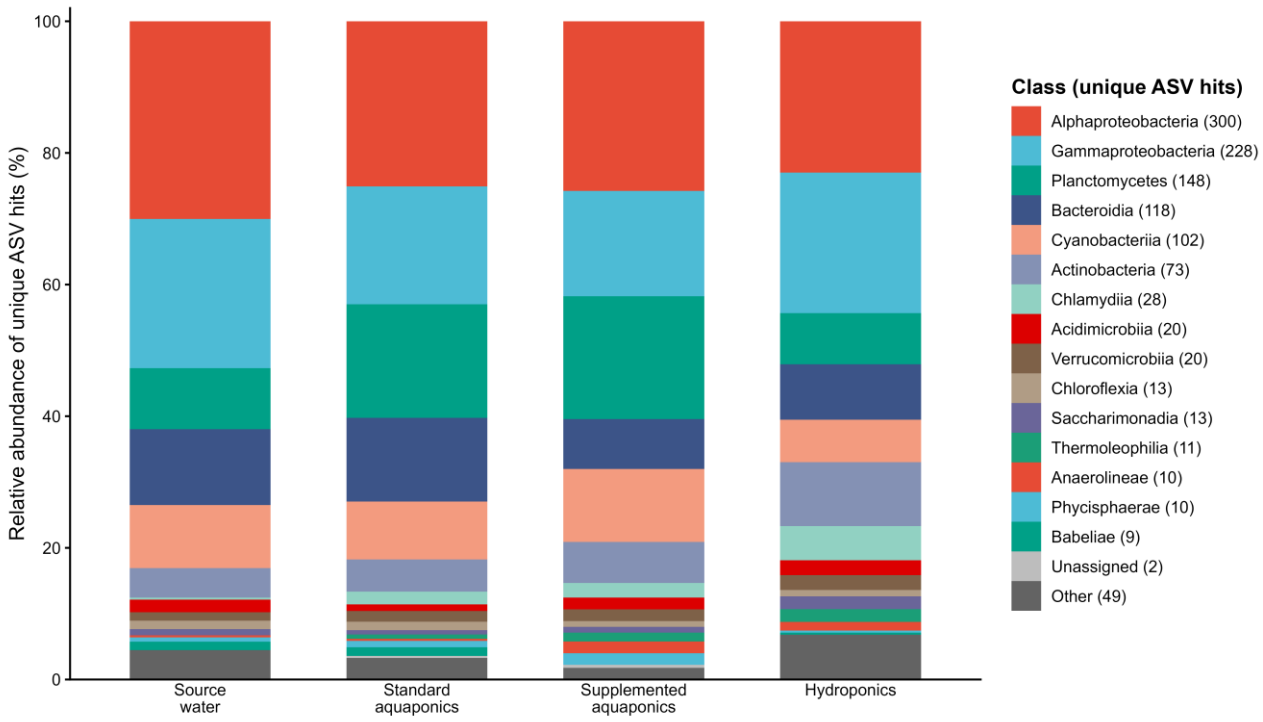


Figure 10. 16S rRNA gene class-level ASV composition by treatment. Stacked bar charts show the relative abundance of unique ASV hits (%) assigned to 16S rRNA class for each treatment.

ITS ASVs were summarized by the class-mapped ecological groups defined in Methods (Figure 11).

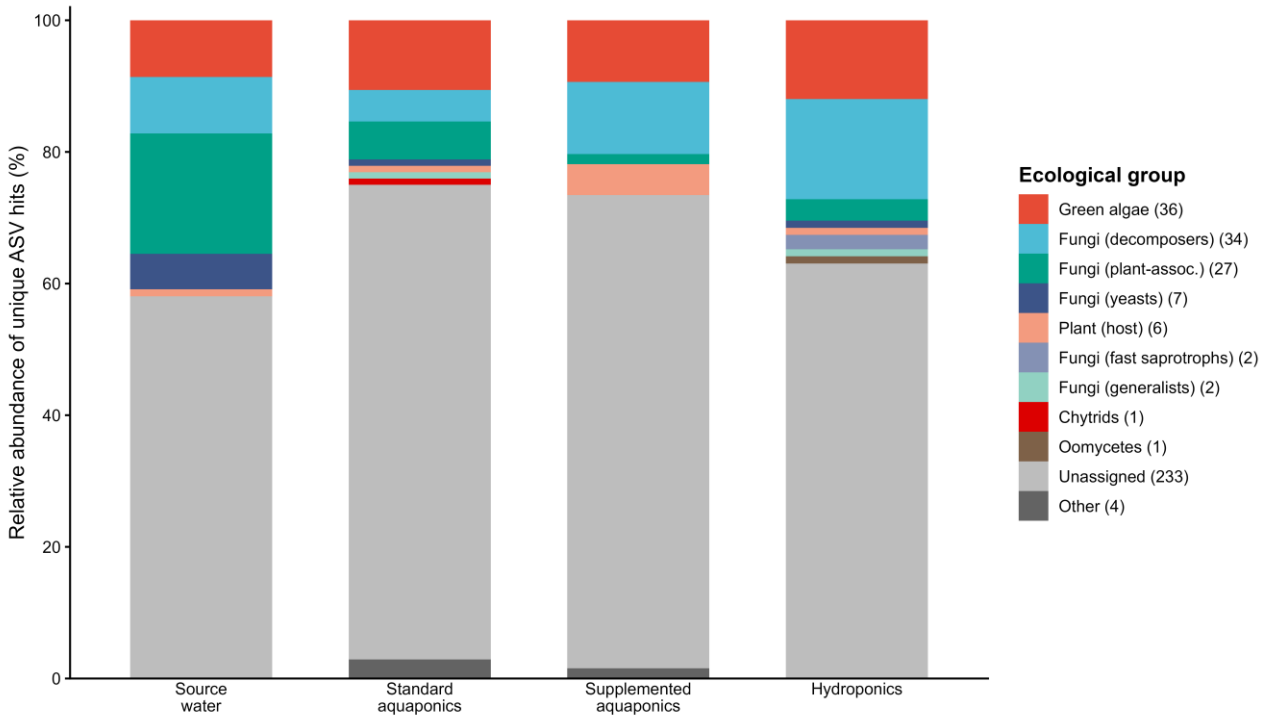


Figure 11. Distribution of ecological groupings associated with each putative class-rank taxonomy across treatment groups.

Nutrient-yield-microbiome integration

Across all nutrients and physicochemical parameters, plant yield showed a strong treatment dependence that was consistent across concentration ranges (Figure 12). Hydroponic plants achieved the highest yields across nearly all nutrients and water parameters, whereas both aquaponic treatments clustered at substantially lower yield levels despite overlapping plant tissue concentrations for most elements. In several cases (e.g., K^+, Ca^{2+}, Mg^{2+}, NO_3^-, PO_4^{3-}, SO_4^{2-}), aquaponic plants spanned similar median tissue concentrations to hydroponic plants but did not approach comparable yield, indicating that adequate tissue nutrient status alone did

not translate into equivalent productivity. Source water plants consistently exhibited the lowest yields and concentrations, reflecting their role as a baseline rather than a productive treatment. These patterns reinforce that yield differences among systems were primarily driven by overall nutrient availability and system-level constraints, rather than by deficiencies in individual measured nutrients at the time of sampling.

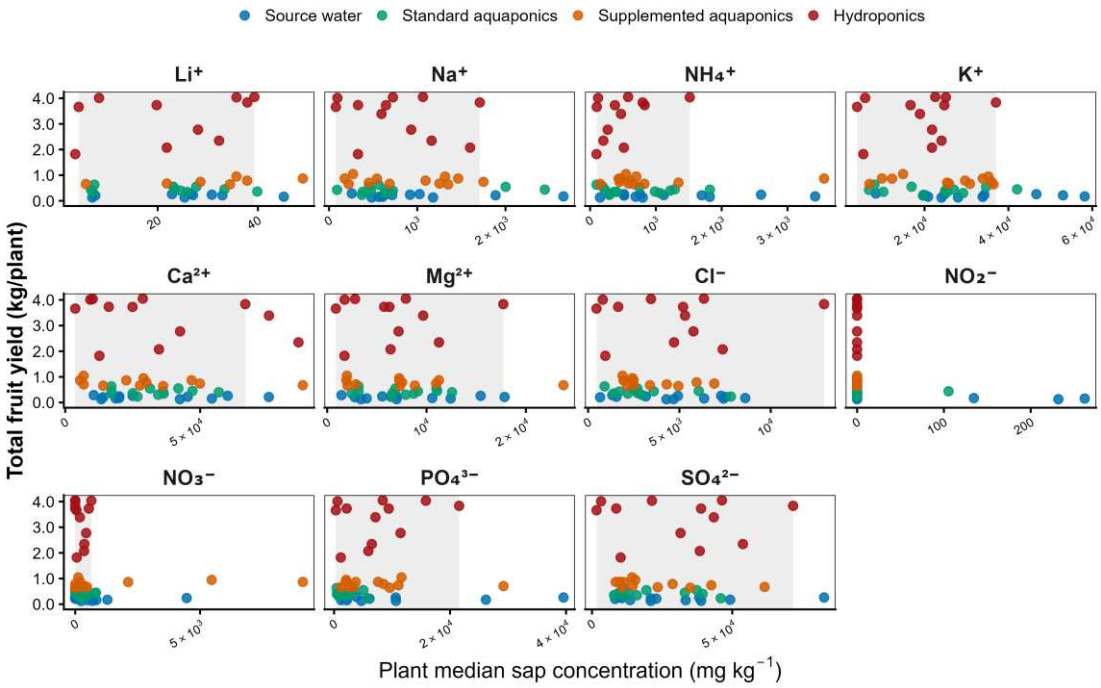


Figure 12. Yield relationships with nutrient and water-quality variables. Each panel shows one nutrient (Li^+, Na^+, NH_4^+, K^+, Ca^{2+}, Mg^{2+}, Cl^-, NO_2^-, NO_3^-, PO_4^{3-}, SO_4^{2-}). Shaded vertical bands indicate the concentration ranges observed among plants achieving ≥90% of the maximum yield recorded across all treatments.

Correlation plots illustrating associations between mean plant sap nutrient concentrations and the relative abundance of a selected ecological group (expressed as a percentage of unique ASVs) are provided in Supplementary Figure S3. Each panel corresponds to a specific nutrient (Na^+, NH_4^+, K^+, Ca^{2+}, Mg^{2+}, NO_2^-, NO_3^-, PO_4^{3-}, and SO_4^{2-}). Points represent treatment-level means. Trend lines indicate the direction of monotonic associations where fitted. Spearman's rank correlation coefficients (ρ) and associated p-values are reported within each panel. A complete list of correlations between each ecological group and nutrient is provided in

Supplementary Tables S1–S4. These tables report results separately for the absolute number of ASVs and for the relative abundance of ASVs (%) in relation to each nutrient.

Across all analyses, significant correlations were exclusively observed for plant sap variables and for water quality variables when expressed as relative percentages of unique ASVs, with no significant relationships detected for water quality based on absolute ASV counts. In the plant sap analyses, yeasts exhibited consistently strong positive correlations (Spearman $\rho = 1.0$, $p = 0.0$) with multiple nutrients, including Na^+, NH_4^+, K^+, Ca^{2+}, Mg^{2+}, and NO_3^-, for both absolute numbers and relative percentages of unique ASVs. Plant-associated fungi showed a strong positive correlation with Ca^{2+} in both absolute and relative sap-based metrics, whereas generalist fungi displayed a significant negative correlation with sap NO_2^- when expressed as relative percentages. In contrast, green algae were negatively correlated with sap PO_4^{3-} for absolute ASV counts, and plant host-associated taxa showed a strong negative correlation with sap Ca^{2+} when using relative percentages. For water quality expressed as relative percentages, generalist fungi were positively correlated with K^+ and NO_2^-, while green algae were negatively correlated with NH_4^+ and Mg^{2+}, suggesting contrasting nutrient associations between fungal generalists and phototrophic taxa in the aqueous environment.

4. Discussion

Aquaponics is frequently framed as a biologically enriched alternative to hydroponics, yet it remains unclear whether this enrichment extends beyond bacterial communities to fungi or how fungal assemblages reorganize under contrasting nutrient regimes. By jointly characterizing root-associated fungal communities, bacterial communities, aqueous nutrient chemistry, plant sap composition, and harvest outcomes, this study links nutrient delivery strategy to plant nutritional status, yield performance, and microbial community structure across four treatments (Figures 1-2). Three consistent patterns emerged. First, fungal

communities exhibited stronger and more structured responses to nutrient regime and supplementation than bacterial communities. Second, targeted nutrient supplementation altered fungal community structure without producing a distinct aquaponics-specific assemblage. Third, fungal diversity and composition varied independently of yield magnitude, indicating that fungal restructuring reflected fertilization type and system configuration more than plant productivity.

4.1. Nutrient regime reorganizes root-associated fungal assemblages

Fungal alpha diversity (ITS) exhibited stronger treatment-specific shifts than bacterial alpha diversity (16S rRNA; cf. Figure 7). Observed fungal richness ranged from 87 ASVs in supplemented aquaponics to 125 ASVs in standard aquaponics, with source water (99 ASVs) and hydroponics (107 ASVs) occupying intermediate positions. Shannon diversity increased from 1.82 in supplemented aquaponics to 2.30 in standard aquaponics and was highest in source water (3.0) and hydroponics (3.06), with Simpson diversity following the same gradient. In published studies of soilless tomato and lettuce systems, ITS Shannon indices typically range from 1.5 to 3.5, with higher values reported under lower nutrient concentrations or organic fertilization regimes (55,56). In contrast, bacterial alpha diversity (16S rRNA gene) varied less across treatments, with Shannon diversity spanning from 2.72 in supplemented aquaponics to 4.27 in standard aquaponics, while hydroponics (4.18) and source water (3.14) were intermediate, and Simpson diversity indicating highest evenness in standard aquaponics (0.96) and hydroponics (0.94) (cf. Figure 7). These values fall within the 2.5-5.0 Shannon range commonly reported for coupled aquaponic and RAS compartments, where typical values cluster around 3.5-4.5 (18–22).

Beta diversity patterns reinforce the asymmetry between bacterial and fungal responses and are consistent with treatment-level differences in taxonomic and ecological composition. In the 16S rRNA gene ordination, standard aquaponics separates primarily along PCoA2, while

hydroponics and supplemented aquaponics cluster closer together and source water separates along PCoA1 (Figure 8). This relatively compact structure among nutrient-supplied treatments aligns with the class-level 16S rRNA gene profiles (Figure 10), which show broadly similar dominant bacterial classes across fertilized systems with only moderate shifts in relative abundance. In contrast, the full ITS ordination exhibits stronger differentiation among nutrient-supplied treatments: source water shifts to the positive side of PCoA1, hydroponics occupies a distinct position along PCoA2, and standard and supplemented aquaponics separate from each other on the negative side of PCoA1 (Figure 8). This greater dispersion among ITS centroids corresponds to clearer treatment-specific differences in fungal class composition (Figure 9) and ecological group structure (Figure 11), indicating that fungal assemblages respond more sensitively to nutrient origin and supplementation than bacterial assemblages. When ITS is restricted to fungi at the kingdom rank, the same treatment relationships become more pronounced (Figure 8). The persistence of this structure in the fungi-only subset suggests that the observed beta-diversity patterns are driven by fungal taxa rather than by non-fungal ITS amplicons.

4.2. Fungal community structure distinguishes aquaponics from hydroponics

Aquaponics did not universally increase fungal diversity relative to hydroponics, but important compositional differences emerged. Hydroponic treatments supported intermediate fungal diversity, comparable to values reported for hydroponic tomato grown on inert substrates without sterilization (55). Across the dataset, the concordance between ordination patterns (cf. Figure 8), class-level composition (cf. Figure 9), and putative ecological group distributions (cf. Figure 11) indicates that nutrient regime effects appeared as compositional reorganization within a shared fungal pool, rather than as discrete, non-overlapping fungal communities. Ordination goodness-of-fit supports this interpretation: Mantel correlations increased from 16S

519 rRNA gene (r = 0.84) to ITS (r = 0.96) and peaked in the fungi-only subset (r = 0.98), indicating
520 that treatment-level structure was captured most faithfully for fungi (cf. Figure 8).
521 This pattern is consistent with evidence from both soil-based and soilless systems showing that
522 sustained nutrient availability restructures fungal community composition without necessarily
523 reducing overall diversity. Long-term nitrogen and phosphorus enrichment typically drives
524 shifts in the relative balance among fungal clades rather than wholesale losses of taxa, resulting
525 in more even communities at the system level (57,58). Phosphorus availability in particular is
526 known to play a key role in modulating plant-associated fungal communities by reducing the
527 relative importance of nutrient-acquisition strategies such as mycorrhizal associations and
528 favoring taxa with broader metabolic flexibility (57,59,60). In this study, ecological group
529 profiles show only subtle compositional differences between standard and supplemented
530 aquaponics (Figure 11), consistent with supplementation acting as a within-regime adjustment
531 rather than a regime shift. Sap phosphate (PO_4^{3-}) was strongly and monotonically associated
532 with the relative contribution of yeast-associated fungi ($\rho = 1.0$), while other fungal groups
533 showed weak or inconsistent responses (Supplementary Tables S1–S4), matching the
534 interpretation that supplementation fine-tuned relative abundances within an already filtered
535 assemblage.
536 A large fraction of ITS ASVs remained unassigned across all systems, reflecting current
537 limitations in fungal reference databases and the likelihood that many aquatic and rhizosphere-
538 associated taxa occupy flexible or poorly characterized ecological roles. When these
539 unassigned ITS ASVs were ordinated separately (Figure 8D), hydroponics separated from
540 aquaponic treatments and source water, mirroring the treatment structure seen for assigned
541 fungal communities (Figure 8B–C). The concordance indicates that unclassified sequences are
542 not randomly distributed with respect to nutrient regime; instead, they carry compositional
543 signal aligned with the broader ITS response to fertilization and water source.(61)

When ecological groups were examined along nutrient gradients, the strongest relationships emerged when abundance was expressed as relative contribution rather than absolute ASV counts (Supplementary Figure S3 and Supplementary Tables S1–S4). Plant-associated fungal groups showed their most consistent positive associations with sap calcium concentrations (Supplementary Figure S3). Calcium plays a central role in plant cell wall stability, membrane integrity, and signaling pathways governing root-microbe interactions (62–64). Variation in calcium availability can therefore indirectly influence fungal colonization by modulating root exudation patterns and host defense responses (65–67). In contrast, decomposer and generalist fungal groups exhibited weaker and less consistent nutrient associations, likely reflecting functional redundancy and metabolic flexibility within these broad categories. Their relative stability across nutrient gradients is consistent with the interpretation that nutrient regime influences which taxa dominate rather than how many fungal taxa are present (Figures 7, 11). Overall, aquaponic and hydroponic treatments do not differ primarily in fungal diversity, but rather in how shared fungal functional groups are redistributed along nutrient gradients and system contexts.

4.3. Plant nutrition and yield contextualize fungal restructuring

Treatment-level aqueous nutrient profiles differed in both magnitude and variability across the cultivation period, establishing a gradient from nutrient-poor source water to a mineral hydroponic positive control, with standard and supplemented aquaponics occupying intermediate positions defined by fish-effluent nutrient origin (Figures 1, 2). Across the experimental duration, pH remained comparatively stable in source water and aquaponic treatments, whereas the hydroponic solution exhibited a progressive decline, consistent with the distinct buffering chemistry and management requirements of mineral nutrient formulations (Figure 3). Electrical conductivity (EC) remained relatively stable within treatments but clearly separated hydroponics from the three low-EC treatments (Figure 4), providing an integrated

indicator of ionic strength and nutrient delivery potential that underpins subsequent plant and yield responses.

This EC gradient was reflected directly in harvest outcomes. Hydroponic plants achieved the highest cumulative yields across cultivars (cf. Figure 6), operating at substantially higher ionic strength than aquaponic treatments (1.78 ± 0.12 mS cm^{-1} versus 0.37-0.41 mS cm^{-1}; cf. Figure 4). The hydroponic EC falls within reported experimental management ranges for tomato nutrient solutions (68,69), whereas aquaponic EC was approximately 75-80% lower than values commonly associated with maximal tomato yield in soilless culture. Within hydroponics, yield variability was largely cultivar-dependent (cf. Figure 6), but across treatments, higher yield was not explained by uniformly higher tissue nutrient concentrations. Plant sap analysis showed substantial overlap in median nutrient concentrations between hydroponic and aquaponic plants (cf. Figure 5), and yield-predictor relationships confirmed that aquaponic plants frequently occupied similar sap concentration ranges to hydroponics without approaching comparable productivity (cf. Figure 12). Together, these patterns indicate that cumulative yield tracked nutrient delivery intensity and flux over time rather than instantaneous tissue concentrations at sampling, explaining why comparable sap composition did not translate into yield convergence under low-EC operation.

Plant sap analysis provides a mechanistic context for this yield pattern. Sap:water heatmaps show that plants maintained strong, ion-specific canopy gradients (notably for calcium and potassium) and temporal structure across sampling dates, with treatment-specific enrichment patterns when normalized to surrounding water chemistry (Figure 5). At the same time, yield-predictor plots demonstrate that aquaponic plants often spanned median tissue concentration ranges overlapping hydroponics for multiple ions (e.g., K^+, Ca^{2+}, Mg^{2+}, NO_3^-, PO_4^{3-}, SO_4^{2-}), yet did not approach comparable yield, indicating that adequate tissue nutrient status alone did not translate into equivalent productivity (Figure 12). These patterns support the interpretation

that nutrient flux and total uptake over time, rather than snapshot tissue concentrations, better predict cumulative fruit production under the conditions tested.

Despite large differences in aqueous nutrient formulations among treatments, plant sap analysis revealed overlapping ranges for several ions across fertilized systems (Figures 1, 5). Across all treatments and sampling dates, calcium concentrations were consistently higher in lower canopy tissues than in upper canopy tissues, whereas potassium showed the opposite vertical pattern (64), particularly during mid- and late-season sampling. The large standard deviations indicate substantial between-plant variability and treatment-specific differences rather than a uniform physiological response. The hydroponic treatment showed reduced separation between canopy levels for some ions in sap:water space, consistent with external supply conditions altering internal mobility rather than uniformly increasing tissue concentrations (cf. Figure 5). Higher nutrient supply therefore increased cumulative tomato production rather than simply increasing nutrient concentrations in fruit or vegetative tissues. Residual differences in mineral concentration between standard and supplemented aquaponics may also reflect differential nutrient uptake and temporal uptake partitioning by plants, although this mechanism could not be resolved within the present study.

4.4. Implications for nutrient optimization in aquaponics

Along the gradient from nutrient excess (hydroponics) to extreme deficiency (source water), the two aquaponic treatments (standard and supplemented) were expected to exhibit intermediate fungal diversity profiles that track fertilization intensity, reflecting an increased reliance on diverse root-associated fungal assemblages under lower nutrient availability. The observed patterns support a more constrained interpretation: aquaponics did not inherently produce higher fungal diversity than hydroponics, and supplementation altered composition more clearly than it altered overall alpha diversity (Figures 7, 11). In practical terms, yield data indicate that microbial complexity did not compensate for the ~75-80% reduction in EC

relative to hydroponic operation, although aquaponic treatments maintained sap nutrient concentrations that frequently overlapped with hydroponics for multiple ions. Yield-nutrient relationships further indicate that high productivity was consistently associated with a narrow range of sap nutrient concentrations (Figure 12), suggesting that proximity to these target nutrient windows is a necessary condition for yield optimization. Under the conditions tested, fungal community restructuring alone was insufficient to offset constraints imposed by low nutrient delivery intensity, indicating that effective aquaponic nutrient management must prioritize achieving and maintaining sap nutrient levels within production-relevant target ranges, irrespective of microbial composition.

From an operational standpoint, these results suggest that monitoring plant sap nutrient concentrations alongside standard water quality parameters provides an additional diagnostic layer for nutrient management decisions in aquaponic systems. The consistent overlap in tissue nutrient concentrations between aquaponic and hydroponic plants, despite a four- to five-fold difference in electrical conductivity, indicates that the nutrient uptake machinery operated comparably across regimes. Yield limitation therefore appears to arise from insufficient cumulative nutrient flux rather than from impaired uptake capacity, supporting management approaches that prioritize sustained nutrient delivery to the root zone rather than replication of the full ionic strength of conventional hydroponic solutions per se.

4.5. Limitations and future directions

The interpretation of fungal community responses in aquaponic and hydroponic systems must be considered in light of several methodological and system-level constraints that also point toward clear priorities for future work. Microbial community structure in aquaponic systems evolves over time, with reported increases in Shannon diversity of 30-60% during the first year of operation (20,70,71). Although the recirculating aquaculture system had been in continuous operation for multiple years, the greenhouse NFT systems were operated only for the duration

of the experiment and therefore may not reflect fully mature rhizosphere communities. The fungal assemblages described here should thus be interpreted as representing early to intermediate successional states.

A second limitation concerns resolution of the ITS dataset. ITS amplicons vary widely in length and sequence composition (72,73) - complicating fixed read-length truncation, standard in 16S rRNA gene workflows - in a way that can disproportionately exclude valid fungal sequences, reducing retained reads and inflating apparent sparsity. Limited reprocessing without strict length assumptions recovered additional sequences, suggesting that part of the low ASV coverage reflects conservative filtering rather than biological absence. Relaxed filtering may weaken error modeling, although this risk is mitigated by the low intrinsic error rate of the Illumina NextSeq platform. Accordingly, diversity metrics reported here should be interpreted as relative indicators of treatment effects rather than exhaustive measures of fungal richness. Future analyses would benefit from sensitivity testing across filtering strategies and from complementary approaches such as longer-read sequencing or absolute quantification. In a similar vein, all diversity metrics are derived from identified ASVs only. Ordination of unassigned ITS ASVs revealed greater similarity between the two aquaponic treatments than between either aquaponics and hydroponics or source water (Figure 8D), suggesting some structural pattern to diversity. Without taxonomic or functional annotation, the ecological significance of this fraction remains uncertain, underscoring the need for improved reference databases and functional assays linking fungal diversity to nutrient transformations and plant performance, especially in CEA systems.

Other ecological factors not explicitly varied in this study may also influence fungal community assembly. Although outside the scope of the present study, substrate type and its physicochemical properties influence the niches available for fungi by structuring microbial microhabitats, resource accessibility, and root-microbe interaction zones (74–77).

Future work should explicitly test interactions among substrate properties, nutrient regime, and microbial succession to clarify how physical and chemical context modulates fungal contributions to nutrient dynamics in soilless cultivation systems. Replacing or complementing amplicon profiling with whole-genome or metagenomic sequencing would also enable more comprehensive characterization of fungal networks, particularly because root-associated fungi in soilless environments remain poorly represented in current reference databases. Finally, a comparison at similar EC or macronutrient concentrations (i.e., nitrogen) would reveal whether the increased microbial load in aquaponics plays a unique role in facilitating plant growth compared to hydroponics, which remains a key question in the field.

5. Conclusions

This study provides the first integrated assessment of fungal diversity, nutrient uptake, and yield performance across hydroponic and aquaponic nutrient regimes. Fungal communities responded sensitively to nutrient origin and supplementation, yet these compositional shifts did not translate into increased productivity under low-EC aquaponic operation. Instead, yield was governed primarily by nutrient delivery intensity and flux, despite substantial overlap in plant sap nutrient concentrations across systems. These findings indicate that aquaponics can restructure root-associated fungal assemblages, but microbial complexity alone is insufficient to offset constraints imposed by reduced nutrient availability. Aligning biological management with production-relevant nutrient targets is therefore essential for improving productivity in soilless cultivation systems.

List of abbreviations

ASV, amplicon sequence variant; CEA, controlled-environment agriculture; EC, electrical conductivity; IC, ion chromatography; IPM, integrated pest management; ITS, internal transcribed spacer; NFT, nutrient film technique; PCoA, principal coordinates analysis;

693 PERMANOVA, permutational multivariate analysis of variance; RAS, recirculating
694 aquaculture system

695 Declarations

696 Ethics approval and consent to participate

697 Not applicable.

698 Consent for publication

699 Not applicable.

700 Competing interests

701 The authors declare that they have no competing interests.

702 Funding

703 This work was supported by the AquaponicsOpti project of Belmont Forum SCP2022, through
704 the Formas grant Joyce 2022-02559 and the German Research Foundation (DFG; grant number
705 516754420), and by the AquaServ transnational access programme (proposal Aquaculture
706 Remineralization for Increased System Efficiency, PID 40879), which enabled access to the
707 INRAe-PEIMA experimental facility.

708 Authors' contributions

709 VL conceived the study, contributed to experimental set-up and harvest, performed the
710 bioinformatic and statistical analyses, and drafted the manuscript. AB, SY, and NL contributed
711 to experimental set-up and monitoring of the aquaculture and hydroponic systems throughout
712 the trial. OK assisted with manuscript editing. AJ supervised the study and revised the
713 manuscript. All authors read and approved the final manuscript.

Availability of data and materials

Raw paired-end 16S rRNA gene and ITS amplicon reads generated during this study have been deposited in the NCBI Sequence Read Archive under BioProject accession PRJNA1465426 (SRA Experiment accessions SRX33369208-SRX33369215; eight SRA Runs SRR38562755-SRR38562762). Per-sample Run accessions are: source water (SAMN59745495) - 16S rRNA gene SRR38562762, ITS SRR38562758; standard aquaponics (SAMN59745496) - 16S rRNA gene SRR38562761, ITS SRR38562757; supplemented aquaponics (SAMN59745497) - 16S rRNA gene SRR38562760, ITS SRR38562756; hydroponics (SAMN59745498) - 16S rRNA gene SRR38562759, ITS SRR38562755. Processed datasets supporting the analyses (plant sap, water-quality, harvest, DADA2 ASV and taxonomy tables, and supplementary correlation tables), together with the R scripts and the R Markdown analysis notebook used to generate the figures and statistical summaries, are archived at Zenodo under https://doi.org/10.5281/zenodo.20511129. Supplementary tables are also provided with this article as Supplementary_tables.xlsx.

Supplementary files

Supplementary_figures.docx. Supplementary Figures S1–S3. Supplementary Figure S1: tomato fruit biomass summary across nutrient regimes. Supplementary Figure S2: cumulative tomato fruit biomass by treatment and cultivar (per-cultivar trajectories with mean ± SD overlay). Supplementary Figure S3: treatment-by-nutrient grid linking mean plant sap nutrient concentrations with plant-associated fungi (% of unique ASVs).

Supplementary_tables.xlsx. Supplementary Tables S1–S4 reporting per-ecogroup correlations of fungal abundance with plant sap (Tables S1, S2) and water (Tables S3, S4) nutrient concentrations, evaluated as absolute ASV counts (Tables S1, S3) and as relative percentages of unique ASVs (Tables S2, S4). The workbook opens with a TOC sheet describing each table.

Acknowledgements

The authors acknowledge collaboration within the AquaponicsOpti project of Belmont Forum SCP2022, including the German project component supported by the German Research Foundation (DFG; grant number 516754420). Access to the INRAe-PEIMA facility was supported by the AquaServ transnational access programme (PID 40879).

References

1. FAO. FAOSTAT: Land Use Database [Internet]. Rome, Italy: Food and Agriculture Organization of the United Nations (FAO); 2023. Available from: https://www.fao.org/faostat/en/#data/RL

2. Foley JA, Ramankutty N, Brauman KA, Cassidy ES, Gerber JS, Johnston M, et al. Solutions for a cultivated planet. Nature. 2011 Oct;478(7369):337–42. doi:10.1038/nature10452

3. Boakes EH, Dalin C, Etard A, Newbold T. Impacts of the global food system on terrestrial biodiversity from land use and climate change. Nat Commun. 2024 Jul 9;15(1):5750. doi:10.1038/s41467-024-49999-z

4. Wheeler T, Von Braun J. Climate Change Impacts on Global Food Security. Science. 2013 Aug 2;341(6145):508–13. doi:10.1126/science.1239402

5. Lesk C, Rowhani P, Ramankutty N. Influence of extreme weather disasters on global crop production. Nature. 2016 Jan;529(7584):84–7. doi:10.1038/nature16467

6. Ortiz-Bobea A, Ault TR, Carrillo CM, Chambers RG, Lobell DB. Anthropogenic climate change has slowed global agricultural productivity growth. Nat Clim Change. 2021 Apr;11(4):306–12. doi:10.1038/s41558-021-01000-1

7. Heuvelink E, Hemming S, Marcelis LFM. Some recent developments in controlled-environment agriculture: on plant physiology, sustainability, and autonomous control. J Hortic Sci Biotechnol. 2025 Sep 3;100(5):604–14. doi:10.1080/14620316.2024.2440592

8. Savvas D, Gruda N. Application of soilless culture technologies in the modern greenhouse industry – A review. Eur J Hortic Sci. 2018 Nov 12;83(5):280–93. doi:10.17660/eJHS.2018/83.5.2

9. Shamshiri RR, Kalantari F, Ting KC, Thorp KR, Hameed IA, Weltzien C, et al. Advances in greenhouse automation and controlled environment agriculture: A transition to plant

factories and urban agriculture. Int J Agric Biol Eng. 2018;11(1):1–22. doi:10.25165/j.ijabe.20181101.3210

10. Chimankare RV, Das S, Kaur K, Magare D. A review study on the design and control of optimised greenhouse environments. J Trop Ecol. 2023;39:e26. doi:10.1017/S0266467423000160

11. Alsanius BW, Wohanka W. Root Zone Microbiology of Soilless Cropping Systems. In: Soilless Culture [Internet]. Elsevier; 2019 [cited 2026 Jul 9]. p. 149–94. Available from: https://linkinghub.elsevier.com/retrieve/pii/B9780444636966000050 doi:10.1016/B978-0-444-63696-6.00005-0

12. Thomas P, Knox OGG, Powell JR, Sindel B, Winter G. The Hydroponic Rockwool Root Microbiome: Under Control or Underutilised? Microorganisms. 2023 Mar 24;11(4):835. doi:10.3390/microorganisms11040835

13. Thomas BO, Lechner SL, Ross HC, Joris BR, Glick BR, Stegelmeier AA. Friends and Foes: Bacteria of the Hydroponic Plant Microbiome. Plants. 2024 Oct 31;13(21):3069. doi:10.3390/plants13213069

14. Yep B, Zheng Y. Aquaponic trends and challenges – A review. J Clean Prod. 2019 Aug;228:1586–99. doi:10.1016/j.jclepro.2019.04.290

15. Choi H, Roy P, Park H, Yang J, Oh SJ, Choi H, et al. Microbial community dynamics and functional shifts in aquaponic systems: Implications for sustainable aquaculture. Aquac Rep. 2025 Dec;45:103248. doi:10.1016/j.aqrep.2025.103248

16. Schmautz Z, Walser JC, Espinal CA, Gartmann F, Scott B, Pothier JF, et al. Microbial diversity across compartments in an aquaponic system and its connection to the nitrogen cycle. Sci Total Environ. 2022 Dec;852:158426. doi:10.1016/j.scitotenv.2022.158426

17. Schmautz Z, Espinal CA, Smits THM, Frossard E, Junge R. Nitrogen transformations across compartments of an aquaponic system. Aquac Eng. 2021 Feb;92:102145. doi:10.1016/j.aquaeng.2021.102145

18. Lobanov V, Keesman KJ, Joyce A. Plants Dictate Root Microbial Composition in Hydroponics and Aquaponics. Front Microbiol. 2022;13:848057. doi:10.3389/fmicb.2022.848057

19. Eck M, Szekely I, Massart S, Jijakli MH. Microorganisms in aquaponics: insights on the composition of the root microbiome of lettuces of varying age. Acta Hortic. 2021 Sep;(1321):213–20. doi:10.17660/ActaHortic.2021.1321.28

20. Schmautz Z, Graber A, Jaenicke S, Goesmann A, Junge R, Smits THM. Microbial diversity in different compartments of an aquaponics system. Arch Microbiol. 2017 May;199(4):613–20. doi:10.1007/s00203-016-1334-1

21. Bartelme RP, Smith MC, Sepulveda-Villet OJ, Newton RJ. Component Microenvironments and System Biogeography Structure Microorganism Distributions in Recirculating Aquaculture and Aquaponic Systems. Tamaki H, editor. mSphere. 2019 Aug 28;4(4):e00143-19. doi:10.1128/mSphere.00143-19

22. Rogge ML, Impullitti AE, Phelps NBD. Metataxonomic Analysis of Microbial Communities in Aquaponic Systems at Two Facilities in the Midwest United States. Bailey C, editor. Aquac Res. 2024 Jan;2024(1):3389398. doi:10.1155/2024/3389398

23. Ruiz A, Andree KB, Furones D, Scicchitano D, Candela M, Carbó R, et al. System design and habitat type drive microbial communities in recirculating aquaculture systems: comparison of conventional fish-only and sustainable aquaponic systems. Front Microbiol. 2026 Feb 24;17:1706522. doi:10.3389/fmicb.2026.1706522

24. Oliveira V, Martins P, Marques B, Cleary DFR, Lillebø AI, Calado R. Aquaponics using a fish farm effluent shifts bacterial communities profile in halophytes rhizosphere and endosphere. Sci Rep. 2020 Jun 22;10(1):10023. doi:10.1038/s41598-020-66093-8

25. Bartelme RP, Oyserman BO, Blom JE, Sepulveda-Villet OJ, Newton RJ. Stripping Away the Soil: Plant Growth Promoting Microbiology Opportunities in Aquaponics. Front Microbiol. 2018 Jan 22;9:8. doi:10.3389/fmicb.2018.00008

26. Delaide B, Delhaye G, Dermience M, Gott J, Soyeurt H, Jijakli MH. Plant and fish production performance, nutrient mass balances, energy and water use of the PAFF Box, a small-scale aquaponic system. Aquac Eng. 2017 Aug;78:130–9. doi:10.1016/j.aquaeng.2017.06.002

27. Goddek S, Vermeulen T. Comparison of Lactuca sativa growth performance in conventional and RAS-based hydroponic systems. Aquac Int. 2018 Dec;26(6):1377–86. doi:10.1007/s10499-018-0293-8

28. Kasozi N, Abraham B, Kaiser H, Wilhelmi B. The complex microbiome in aquaponics: significance of the bacterial ecosystem. Ann Microbiol. 2021 Dec;71(1):1. doi:10.1186/s13213-020-01613-5

29. Kasozi N, Tandlich R, Fick M, Kaiser H, Wilhelmi B. Iron supplementation and management in aquaponic systems: A review. Aquac Rep. 2019 Nov;15:100221. doi:10.1016/j.aqrep.2019.100221

30. Wongkiew S, Hu Z, Chandran K, Lee JW, Khanal SK. Nitrogen transformations in aquaponic systems: A review. Aquac Eng. 2017 Jan;76:9–19. doi:10.1016/j.aquaeng.2017.01.004

31. Wongkiew S, Park MR, Chandran K, Khanal SK. Aquaponic Systems for Sustainable Resource Recovery: Linking Nitrogen Transformations to Microbial Communities. Environ Sci Technol. 2018 Nov 6;52(21):12728–39. doi:10.1021/acs.est.8b04177

32. Lobanov VP, Combot D, Pelissier P, Labbé L, Joyce A. Improving Plant Health Through Nutrient Remineralization in Aquaponic Systems. Front Plant Sci. 2021;12. doi:10.3389/fpls.2021.683690

33. Tellbüscher AA, Van Hullebusch E, Gebauer R, Mráz J. Assessing the fate and behaviour of plant nutrients in aquaponic systems by chemical equilibrium modelling: A meta-analytical approach. Water Res. 2024 Oct;264:122226. doi:10.1016/j.watres.2024.122226

34. Yang T, Kim HJ. Comparisons of nitrogen and phosphorus mass balance for tomato-, basil-, and lettuce-based aquaponic and hydroponic systems. J Clean Prod. 2020 Nov;274:122619. doi:10.1016/j.jclepro.2020.122619

35. Utkhede R. Increased Growth and Yield of Hydroponically Grown Greenhouse Tomato Plants Inoculated with Arbuscular Mycorrhizal Fungi and Fusarium oxysporum f. sp. radicis-lycopersici. Biocontrol. 2006 Jun;51(3):393–400. doi:10.1007/s10526-005-4243-9

36. Kowalska I, Konieczny A, Gąstoł M, Sady W, Hanus-Fajerska E. Effect of mycorrhiza and phosphorus content in nutrient solution on the yield and nutritional status of tomato plants grown on rockwool or coconut coir. Agric Food Sci. 2015 Mar 20;24(1):39–51. doi:10.23986/afsci.47204

37. Robinson Boyer L, Feng W, Gulbis N, Hajdu K, Harrison RJ, Jeffries P, et al. The Use of Arbuscular Mycorrhizal Fungi to Improve Strawberry Production in Coir Substrate. Front Plant Sci. 2016 Aug 19;7. doi:10.3389/fpls.2016.01237

38. Duan S, Feng G, Limpens E, Bonfante P, Xie X, Zhang L. Cross-kingdom nutrient exchange in the plant–arbuscular mycorrhizal fungus–bacterium continuum. Nat Rev Microbiol. 2024 Dec;22(12):773–90. doi:10.1038/s41579-024-01073-7

39. Zhang C, Van Der Heijden MGA, Dodds BK, Nguyen TB, Spooren J, Valzano-Held A, et al. A tripartite bacterial-fungal-plant symbiosis in the mycorrhiza-shaped microbiome drives plant growth and mycorrhization. Microbiome. 2024 Jan 19;12(1):13. doi:10.1186/s40168-023-01726-4

40. Caser M, Demasi S, Victorino ÍMM, Donno D, Faccio A, Lumini E, et al. Arbuscular Mycorrhizal Fungi Modulate the Crop Performance and Metabolic Profile of Saffron in Soilless Cultivation. Agronomy. 2019 May 8;9(5):232. doi:10.3390/agronomy9050232

41. Sonneveld C, Voogt W. Plant Nutrition of Greenhouse Crops [Internet]. Dordrecht: Springer Netherlands; 2009 [cited 2026 Jul 9]. Available from: http://link.springer.com/10.1007/978-90-481-2532-6 doi:10.1007/978-90-481-2532-6

42. Esteves E, Locatelli G, Bou NA, Ferrarezi RS. Sap Analysis: A Powerful Tool for Monitoring Plant Nutrition. Horticulturae. 2021 Oct 22;7(11):426. doi:10.3390/horticulturae7110426

43. Gorham J. Analysis of Inorganic Anions And Cations In Plant Tissues By Ion Chromatography. In: Williams PA, Hudson MJ, editors. Recent Developments in Ion Exchange [Internet]. Dordrecht: Springer Netherlands; 1987 [cited 2026 Jul 9]. p. 14–21. Available from: http://link.springer.com/10.1007/978-94-009-3449-8_2 doi:10.1007/978-94-009-3449-8_2

44. Sonneveld C. Nutrient solutions for vegetables and flowers grown in water or substrates. Naaldwijk: Proefstation voor Tuinbouw onder Glas; 1983.

45. Novaes HB, Vaitsman DS, Dutra PB, Pérez DV. Determination of nitrate in lettuce by ion chromatography after microwave water extraction. Quím Nova. 2009;32(6):1647–50. doi:10.1590/S0100-40422009000600049

886 46. Klindworth A, Pruesse E, Schweer T, Peplies J, Quast C, Horn M, et al. Evaluation of
887 general 16S ribosomal RNA gene PCR primers for classical and next-generation
888 sequencing-based diversity studies. Nucleic Acids Res. 2013 Jan 1;41(1):e1–e1.
889 doi:10.1093/nar/gks808

890 47. Ihrmark K, Bödeker ITM, Cruz-Martinez K, Friberg H, Kubartova A, Schenck J, et al. New
891 primers to amplify the fungal ITS2 region - evaluation by 454-sequencing of artificial and
892 natural communities. FEMS Microbiol Ecol. 2012 Dec;82(3):666–77. doi:10.1111/j.1574-
893 6941.2012.01437.x

894 48. White TJ, Bruns T, Lee S, Taylor J. AMPLIFICATION AND DIRECT SEQUENCING
895 OF FUNGAL RIBOSOMAL RNA GENES FOR PHYLOGENETICS. In: PCR Protocols
896 [Internet]. Elsevier; 1990 [cited 2026 Jul 9]. p. 315–22. Available from:
897 https://linkinghub.elsevier.com/retrieve/pii/B9780123721808500421 doi:10.1016/B978-
898 0-12-372180-8.50042-1

899 49. Callahan BJ, McMurdie PJ, Rosen MJ, Han AW, Johnson AJA, Holmes SP. DADA2:
900 High-resolution sample inference from Illumina amplicon data. Nat Methods. 2016
901 Jul;13(7):581–3. doi:10.1038/nmeth.3869

902 50. McMurdie PJ, Holmes S. phyloseq: An R Package for Reproducible Interactive Analysis
903 and Graphics of Microbiome Census Data. Watson M, editor. PLoS ONE. 2013 Apr
904 22;8(4):e61217. doi:10.1371/journal.pone.0061217

905 51. Ondov BD, Bergman NH, Phillippy AM. Interactive metagenomic visualization in a Web
906 browser. BMC Bioinformatics. 2011 Dec;12(1):385. doi:10.1186/1471-2105-12-385

907 52. Nilsson RH, Tedersoo L, Ryberg M, Kristiansson E, Hartmann M, Unterseher M, et al. A
908 Comprehensive, Automatically Updated Fungal ITS Sequence Dataset for Reference-
909 Based Chimera Control in Environmental Sequencing Efforts. Microbes Environ.
910 2015;30(2):145–50. doi:10.1264/jsme2.ME14121

911 53. Anderson MJ. A new method for non-parametric multivariate analysis of variance. Austral
912 Ecol. 2001 Feb;26(1):32–46. doi:10.1046/j.1442-9993.2001.01070.x

913 54. Oksanen J, Simpson GL, Blanchet FG. vegan: Community Ecology Package [Internet]. R
914 package; 2025. Available from: https://CRAN.R-project.org/package=vegan

915 55. Grunert O, Robles-Aguilar AA, Hernandez-Sanabria E, Schrey SD, Reheul D, Van Labeke
916 MC, et al. Tomato plants rather than fertilizers drive microbial community structure in
917 horticultural growing media. Sci Rep. 2019 Jul 2;9(1):9561. doi:10.1038/s41598-019-
918 45290-0

919 56. Grunert O, Reheul D, Van Labeke M, Perneel M, Hernandez-Sanabria E, Vlaeminck SE,
920 et al. Growing media constituents determine the microbial nitrogen conversions in organic
921 growing media for horticulture. Microb Biotechnol. 2016 May;9(3):389–99.
922 doi:10.1111/1751-7915.12354

923 57. Lekberg Y, Arnillas CA, Borer ET, Bullington LS, Fierer N, Kennedy PG, et al. Nitrogen
924 and phosphorus fertilization consistently favor pathogenic over mutualistic fungi in
925 grassland soils. Nat Commun. 2021 Jun 9;12(1):3484. doi:10.1038/s41467-021-23605-y

58. Morrison EW, Frey SD, Sadowsky JJ, Van Diepen LTA, Thomas WK, Pringle A. Chronic nitrogen additions fundamentally restructure the soil fungal community in a temperate forest. Fungal Ecol. 2016 Oct;23:48–57. doi:10.1016/j.funeco.2016.05.011

59. Miao F, Wang S, Yuan Y, Chen Y, Guo E, Li Y. The Addition of a High Concentration of Phosphorus Reduces the Diversity of Arbuscular Mycorrhizal Fungi in Temperate Agroecosystems. Diversity. 2023 Sep 28;15(10):1045. doi:10.3390/d15101045

60. Long XE, Yao H. Phosphorus Input Alters the Assembly of Rice (Oryza sativa L.) Root-Associated Communities. Microb Ecol. 2020 Feb;79(2):357–66. doi:10.1007/s00248-019-01407-6

61. Nilsson RH, Anslan S, Bahram M, Wurzbacher C, Baldrian P, Tedersoo L. Mycobiome diversity: high-throughput sequencing and identification of fungi. Nat Rev Microbiol. 2019 Feb;17(2):95–109. doi:10.1038/s41579-018-0116-y

62. Bhar A, Chakraborty A, Roy A. The captivating role of calcium in plant-microbe interaction. Front Plant Sci. 2023 Mar 3;14:1138252. doi:10.3389/fpls.2023.1138252

63. Lecourieux D, Ranjeva R, Pugin A. Calcium in plant defence-signalling pathways. New Phytol. 2006 Jul;171(2):249–69. doi:10.1111/j.1469-8137.2006.01777.x

64. Marschner H. Mineral Nutrition and Yield Response. In: Mineral Nutrition of Higher Plants [Internet]. Elsevier; 1995 [cited 2026 Jul 9]. p. 184–200. Available from: https://linkinghub.elsevier.com/retrieve/pii/B9780124735422500080 doi:10.1016/B978-012473542-2/50008-0

65. Zhang L, Du L, Poovaiah BW. Calcium signaling and biotic defense responses in plants. Plant Signal Behav. 2014 Nov 2;9(11):e973818. doi:10.4161/15592324.2014.973818

66. Camli-Saunders D, Villouta C. Root exudates in controlled environment agriculture: composition, function, and future directions. Front Plant Sci. 2025 Apr 28;16:1567707. doi:10.3389/fpls.2025.1567707

67. Sasse J, Martinoia E, Northen T. Feed Your Friends: Do Plant Exudates Shape the Root Microbiome? Trends Plant Sci. 2018 Jan;23(1):25–41. doi:10.1016/j.tplants.2017.09.003

68. Dorai M, Papadopoulos AP, Gosselin A. Influence of electric conductivity management on greenhouse tomato yield and fruit quality. Agronomie. 2001 May;21(4):367–83. doi:10.1051/agro:2001130

69. Ou X, Liu D, Liu A, Liu H, Chen R, Zhang Y. Effects of nutrient solution management modes on fruit production and quality of tomatoes grown in extremely root restriction. Sci Hortic. 2023 Nov;321:112366. doi:10.1016/j.scienta.2023.112366

70. Eck M, Sare AR, Massart S, Schmautz Z, Junge R, Smits THM, et al. Exploring Bacterial Communities in Aquaponic Systems. Water. 2019 Feb 2;11(2):260. doi:10.3390/w11020260

71. Wang Z, Li T, Wen X, Liu Y, Han J, Liao Y, et al. Fungal Communities in Rhizosphere Soil under Conservation Tillage Shift in Response to Plant Growth. Front Microbiol. 2017 Jul 11;8:1301. doi:10.3389/fmicb.2017.01301

72. Pauvert C, Buée M, Laval V, Edel-Hermann V, Fauchery L, Gautier A, et al. Bioinformatics matters: The accuracy of plant and soil fungal community data is highly dependent on the metabarcoding pipeline. Fungal Ecol. 2019 Oct;41:23–33. doi:10.1016/j.funeco.2019.03.005

73. Edgar RC. Accuracy of taxonomy prediction for 16S rRNA and fungal ITS sequences. PeerJ. 2018 Apr 18;6:e4652. doi:10.7717/peerj.4652

74. Bardgett RD, Van Der Putten WH. Belowground biodiversity and ecosystem functioning. Nature. 2014 Nov;515(7528):505–11. doi:10.1038/nature13855

75. Rousk J, Bååth E, Brookes PC, Lauber CL, Lozupone C, Caporaso JG, et al. Soil bacterial and fungal communities across a pH gradient in an arable soil. ISME J. 2010 Oct 1;4(10):1340–51. doi:10.1038/ismej.2010.58

76. Fierer N. Embracing the unknown: disentangling the complexities of the soil microbiome. Nat Rev Microbiol. 2017 Oct;15(10):579–90. doi:10.1038/nrmicro.2017.87

77. Gruda N. Increasing Sustainability of Growing Media Constituents and Stand-Alone Substrates in Soilless Culture Systems. Agronomy. 2019 Jun 9;9(6):298. doi:10.3390/agronomy9060298

Supplementary Files

This is a list of supplementary files associated with this preprint. Click to download.

- Supplementarytables.xlsx
- Supplementaryfigures.docx